

# Flux and grain size variation of eolian dust as a proxy tool for the paleo-position of the Intertropical Convergence Zone in the northeast Pacific

Kiseong Hyeong\*, Chan Min Yoo, Jonguk Kim, Sang-Bum Chi, Ki-Hyune Kim

*Deep-sea Resources Research Center, Korea Ocean Research Development Institute, Ansan P.O. Box 29, Seoul 425-600, South Korea*

Received 31 May 2005; received in revised form 20 February 2006; accepted 16 March 2006

## Abstract

A 328 cm-long piston core (KODOS 02-01-02) collected from the northeast equatorial Pacific at 16°12'N, 125°59'W was investigated for eolian mass fluxes and grain sizes to test these proxies as a tool for the paleo-position of the Intertropical Convergence Zone (ITCZ). The eolian mass fluxes of the lower interval below 250 cm (15.5–7.6 Ma) are very uniform at  $5 \pm 1 \text{ mg/cm}^2/10^3 \text{ yr}$ , while those of the upper interval above 250 cm (from 7.6 Ma) are over 2 times higher than the lower interval at  $12 \pm 1 \text{ mg/cm}^2/10^3 \text{ yr}$ . The median grain size of the eolian dusts in the lower interval increases from  $8.4\phi$  to  $8.0\phi$  downward, while that of the upper interval varies in a narrow range from  $8.8\phi$  to  $8.6\phi$ . The determined values compare well in magnitude to those of central Pacific sediments for the upper interval and equatorial and southeast Pacific sediments for the lower interval. This result suggests a possibility that the study site had been under the influence of southeast trade winds at its earlier depositional period due to the northerly position of the ITCZ, and subsequently of the northeast trade winds for a later period when the upper sediments were deposited. This interpretation is consistent with a mineralogical and geochemical study published elsewhere that assigned the provenance of the study core dust to Central/South America for the lower interval and to Asia for the upper interval. This study suggests that the distinct differences in eolian mass flux and grain size observed across the ITCZ can be used to trace the paleo-latitude of the ITCZ.

© 2006 Elsevier B.V. All rights reserved.

*Keywords:* Intertropical Convergence Zone; Mass accumulation rate; Grain size; Eolian dust; Northeast Pacific; Pelagic sediments

## 1. Introduction

The Intertropical Convergence Zone (ITCZ), the place where the southeast and northeast trade winds meet, is an important climatic component that reflects the tropical atmospheric circulation pattern (Pisias and Mix, 1997). The ITCZ shifts in its latitudinal position

depending on the relative strength of the northeast and southeast trade winds, which is in turn controlled by the temperature gradient between pole and equator in each hemisphere (Flohn, 1981; Hovan, 1995; Pisias and Mix, 1997). Flohn (1981) suggested that the ITCZ was located at around 12°N during the late Tertiary, farther north than its present annually averaged position of ~6°N. It was attributed to a much stronger temperature gradient between pole and equator in the southern hemisphere under the late Tertiary situation of an ice-free Arctic and Antarctic ice-cap volume similar to or even greater than that of today. This theoretical

\* Corresponding author. Tel.: +82 31 400 6382; fax: +82 31 418 8772.

E-mail address: [kshyeong@kordi.re.kr](mailto:kshyeong@kordi.re.kr) (K. Hyeong).

estimation was documented in many deep-sea sedimentary cores through the investigation of down-core variations in source regimes, eolian dust fluxes, and grain size distributions (Kyte et al., 1993; Rea, 1994; Hovan, 1995; Lyle et al., 2002; Pettke et al., 2002; Vanden Berg and Jarrard, 2004; Hyeong et al., 2005).

The ITCZ separates northern and southern hemispheres in dust deposition because of associated heavy rainfall and resulting washing-out of dust particles from the atmosphere (Merrill et al., 1989; Rea, 1994; Hovan, 1995; Pettke et al., 2002; Vanden Berg and Jarrard, 2004). As a result, north of the ITCZ, surface sediments are dominated by China loess transported by the zonal westerlies and northeast trade winds while, south of the ITCZ, sediments are dominated by Central/South American dust transported by the southeast trade winds (Griffin and Goldberg, 1963; Corliss et al., 1982; Merrill et al., 1989; Olivarez et al., 1991; Nakai et al., 1993; Jones et al., 1994). Thus the paleo-location of the ITCZ can be delineated by distinguishing these sources through the investigation of down-core variation in mineralogical, geochemical, and isotopic composition of eolian components in deep-sea cores (Rea, 1994; Pettke et al., 2002; Lyle et al., 2002; Hyeong et al., 2005).

For example, Rea (1994) interpreted the transition in mineralogy, chemistry, and flux in central north Pacific core LL44-GPC3 as a result of ITCZ position far to the north of its present position during the Early Neogene. Based on the Nd isotope composition of the same core, Pettke et al. (2002) documented a northerly position of the ITCZ during the Cenozoic and suggested an ITCZ location of  $\sim 23^\circ\text{N}$  at around 40 Ma. Lyle et al. (2002) reached similar conclusions but proposed a further north position of the ITCZ at  $\sim 27^\circ\text{N}$  at around 20 Ma and moving southward since then, based on shifts in mineralogy from illite-rich to smectite-rich composition in ODP Leg 199 cores. Hyeong et al. (2005) investigated mineral and geochemical composition of KODOS 02-01-02 core from the northeast Pacific and proposed the paleo-latitude of the ITCZ at around  $12^\circ\text{N}$  during the Late Miocene.

The ITCZ can also be traced by means of eolian fluxes and grain size variations (Rea, 1994; Hovan, 1995; Vanden Berg and Jarrard, 2004). High rainfall and efficient removal of dust particles in the ITCZ result in an increased flux of eolian sediments to the pelagic ocean beneath it. Conversely, atmospheric circulation intensity is weakest in the ITCZ and increases toward the trade winds regime to the north and south (Wyrski and Kilonsky, 1984), resulting in an accumulation of the finest dust material beneath the ITCZ and a coarsening of it to the south and north away from the ITCZ (Hovan, 1995). Thus, the paleo-position of the ITCZ may be recorded in the form of increased dust

flux and decreased grain size in deep-sea cores and can be traced by investigating down-core variation of these two proxy data. Using them, for example, Hovan (1995) estimated the paleo-latitude of the ITCZ to be north of  $7^\circ\text{N}$  during the latest Miocene in the east Pacific. However, Vanden Berg and Jarrard (2004) suggested a relatively fixed location of the ITCZ centered near the equator since the Eocene using the same approach.

Besides the grain size distribution and eolian flux variation directly associated with the ITCZ, careful examination of the existing data reveals a significant difference in eolian fluxes and grain sizes of Pacific sediments across the ITCZ (Rea and Janecek, 1982; Janecek and Rea, 1983, 1985; Janecek, 1985; Bloomstine and Rea, 1986; Rea and Bloomstine, 1986; Chuey et al., 1987; Rea, 1994; Rea et al., 1994; Rea and Hovan, 1995). Present-day dust fluxes in the eastern Pacific, for example, fall by 1 to 2 orders of magnitude from north to south across the ITCZ while median grain size shows about  $1\phi$  to  $2\phi$  increase from north to south. Such contrasts in eolian flux and grain size between the south and north Pacific were found to have been maintained since early Oligocene. These temporal and spatial variations of eolian flux and grain size distribution across the ITCZ are due to the changes in availability of dust materials in source regimes and differences in intensities of zonal wind systems that carry the dust particles (Parkin and Shackleton, 1973; Rea, 1982; Rea and Janecek, 1982; Rea et al., 1985; Rea, 1994). It implies, not tested yet, that the large contrast in MARs and grain size of eolian dust observed across the ITCZ might be used to trace the paleo-position of the ITCZ in deep-sea cores.

This study aims at the documentation of transition in mass flux and grain size distribution of eolian dusts, correlated with a corresponding source change, as a proxy tool for tracing the ITCZ. For this, we investigated the mass flux and grain size of eolian dust in a piston core (KODOS 02-01-02) that was dominantly recording down-core variation of source regimes from northern to southern hemispheres across the ITCZ. The combination of the techniques of physical and geochemical characterization of the eolian dust component provides a powerful tool for the interpretation of pelagic sediment sources and tracing of the ITCZ.

## 2. Study area

A 328 cm-long piston core (KODOS 02-01-02) was collected from  $16^\circ 12'\text{N}$ ,  $125^\circ 59'\text{W}$  at 4550 m water depth in the region between the Clarion and Clipperton (C–C) Fracture Zones of the northeast Equatorial Pacific (Fig. 1). The coring site is more than 2000 km west

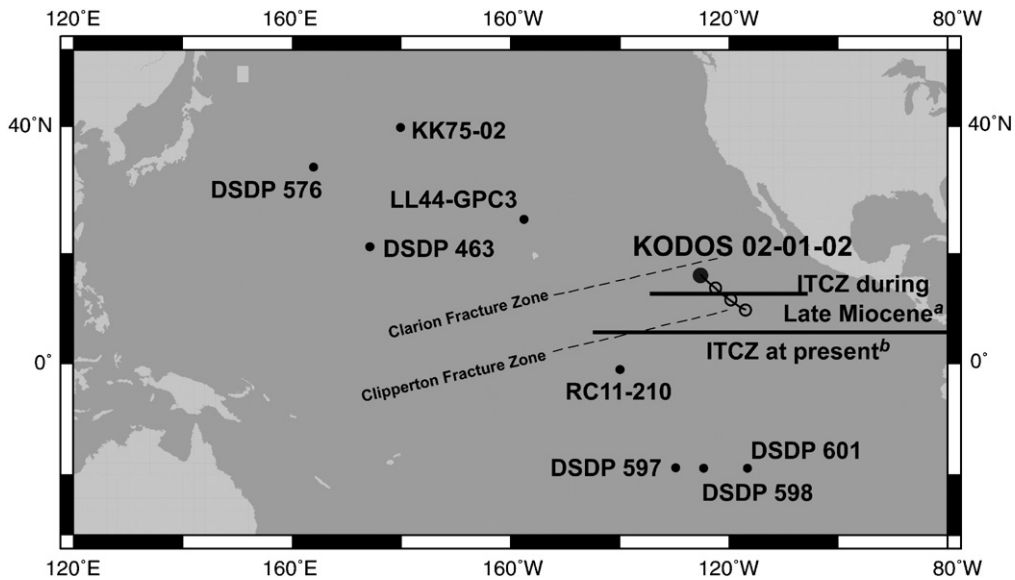


Fig. 1. Site locations of the study core (KODOS 02-01-02) and other cores discussed in the study. The locations of the cores other than the study site are Rea and Janecek (1982), Janecek and Rea (1983, 1985), Bloomstine and Rea (1986), Janecek (1985), and Chuey et al. (1987). Open symbols represent the backtrack path of the study site with increments of 5 Myr (<http://odsn.de/odsn/services/paleomap/paleomap.html>, based on the work of Hay et al., 1999). The proposed paleo-locations of the ITCZ proposed are shown as horizontal lines: a, Hyeong et al. (2005) and b, Pettke et al. (2002).

of the East Pacific Rise and Central America, and thus likely devoid of hemipelagic sedimentation (e.g. Rea, 1994). Calcareous oozes and marls dominate surface sediments south of the Clipperton Fracture Zone, but are

replaced with siliceous ooze and pelagic red clay in the region to the north with increasing water depth and shallowing of carbonate compensation depth from 4800 to 4400 m (Piper et al., 1979; Muller et al., 1988). The

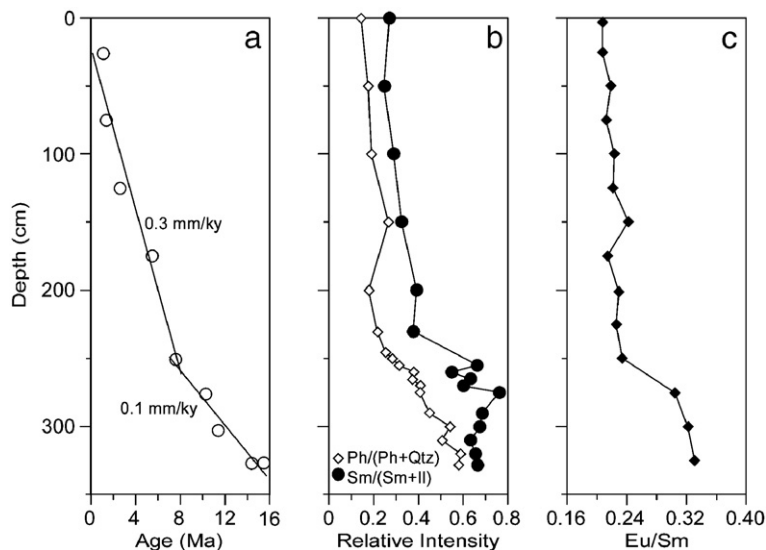


Fig. 2. Plots of age (a), mineral composition (b), and Eu/Sm ratios (c) against depth of the study core. Data are from Hyeong et al. (2005). Age was determined from Sr isotope ratios of fish teeth. Ph, Qtz, Sm, and Il stand for phillipsite, quartz, smectite, and illite, respectively. Smectite/illite ratios were calculated for peak areas and phillipsite/quartz for peak intensities. A factor of 4 was multiplied to the area of illite peak for smectite/illite ratios (Biscaye, 1965).

C–C region shows a zonal sediment distribution pattern of siliceous ooze and pelagic red clay roughly in a N–S direction, but the northeastern part of the C–C zone, where the coring site is located, is dominated by pelagic red clays (Muller et al., 1988). Sedimentation rates vary over a wide range from less than 0.5 mm/10<sup>3</sup> yr to several mm/10<sup>3</sup> yr in the C–C region, largely depending on sediment types (Piper and Williamson, 1977; Theyer, 1977; Muller and Mangini, 1980; Muller et al., 1988). In general, sedimentation rates are higher for calcareous ooze in the south and lower for red clays in the northern part of the C–C region, thus decrease northward. Local redistribution of fine material due to bottom currents may play a minor role in local scale variation in sedimentation rates (Piper and Blueford, 1982; Muller et al., 1988). The seafloor of the study area is covered with abundant manganese nodules, more than 5 kg/m<sup>2</sup> (Jeong et al., 1994; Jung et al., 1998).

### 3. Description and source regime of the study core

The core sediments consist of slightly bioturbated homogeneous pelagic clays and are divided into two intervals based on a distinct color change; an upper interval above 250 cm composed of dark brown sediments and a lower interval of yellowish-brown sediments below 250 cm to the bottom of the core (328 cm), hereafter called “upper and lower intervals”, respectively. The lower interval sediments show lower water contents and include more micro-manganese nodules than the upper interval.

The upper and lower intervals are also distinctive in the mineralogical and geochemical compositions of eolian components. The eolian components below 250 cm are characterized by smectite- and phillipsite-rich mineral composition, depleted heavy REEs ((La/Yb)<sub>CN</sub>=6.3), and high Eu/Sm ratios (0.30–0.33) (Fig. 2), indicative of volcanic-rich composition (Hyeong et al., 2005). These characteristics are found in equatorial and south Pacific surface sediments, of which eolian particles are supplied from volcanic arcs and young continental crusts of Central/South America (Griffin and Goldberg, 1963; Corliss et al., 1982; Olivarez et al., 1991; Nakai et al., 1993; Jones et al., 1994; Weber et al., 1996; Jones et al., 2000; Lyle et al., 2002). In contrast, eolian components of the upper interval are characterized by quartz- and illite-rich mineralogy, and more shale-like REE and trace element compositions (Fig. 2) (Hyeong et al., 2005), which are common in surface sediments of the central Pacific north of the ITCZ, where eolian particles are mainly derived from Asia (Griffin and Goldberg, 1963; Corliss et al., 1982; Olivarez et al., 1991; Kyte et al., 1993; Nakai et al., 1993; Rea, 1994; Weber et al., 1996; Lyle et al., 2002).

The hemispheric source change from Central/South America to Asia now occurs across the hemispheric dust barrier of the ITCZ. It has been proposed that the ITCZ was located at ~27°N at around 20 Ma and shifted southward toward its present position since then (Rea, 1994; Lyle et al., 2002; Pettke et al., 2002). Thus, the observed hemispheric source change is likely attributed to the northerly position of the ITCZ during late Miocene, when the hemispheric source change was recorded in the study core (Hyeong et al., 2005). Backtrack path construction of Pacific plate (<http://odsn.de/odsn/services/paleomap/paleomap.html>, based on the work of Hay et al., 1999) indicated paleo-location of the ITCZ north of 12°N (±2°) prior to late Miocene (Hyeong et al., 2005) (Fig. 1).

### 4. Methods

Sub-samples were taken at 1 cm intervals from the split core on board ship and stored in a refrigerator for

Table 1  
Data for calculation of eolian mass accumulation rates

Depth (cm)	Age (Ma)	Porosity (%)	DBD (g/cm <sup>3</sup> )	LSR (cm/10 <sup>3</sup> yr)	MAR (mg/cm <sup>2</sup> /10 <sup>3</sup> yr)	Eolian (wt.%)	Eolian MAR (mg/cm <sup>2</sup> /10 <sup>3</sup> yr)
3	0.1	86.2	0.43	0.032	13.7	67.3	9.2
16	0.6	77.8	0.58	0.032	18.5	66.9	12.3
36	1.1	76.7	0.61	0.032	19.4	68.0	13.2
50	1.2	77.3	0.59	0.032	18.8	62.1	11.7
62	1.3	77.9	0.57	0.032	18.2	63.2	11.5
75	1.4	77.6	0.58	0.032	18.5	66.4	12.3
87	1.6	77.1	0.59	0.032	18.8	67.2	12.6
100	2.0	76.6	0.60	0.032	19.1	68.5	13.1
112	2.2	77.2	0.59	0.032	18.8	67.7	12.7
137	3.2	76.9	0.59	0.032	18.8	66.5	12.5
162	4.6	74.3	0.58	0.032	18.5	60.3	11.1
175	5.4	75.1	0.62	0.032	19.7	58.2	11.5
187	5.8	75.0	0.65	0.032	20.7	67.1	13.9
201	6.2	75.1	0.64	0.032	20.4	58.9	12.0
212	6.5	75.4	0.63	0.032	20.1	66.5	13.3
225	6.8	75.0	0.64	0.032	20.4	65.3	13.3
237	7.2	73.4	0.68	0.032	21.7	43.3	9.4
250	7.5	73.4	0.68	0.032	21.7	64.1	13.9
255	8.0	72.7	0.69	0.011	7.6	66.4	5.0
262	8.7	72.0	0.71	0.011	7.8	66.7	5.2
265	9.0	72.1	0.71	0.011	7.8	66.1	5.2
272	9.8	72.1	0.71	0.011	7.8	65.2	5.1
275	10.1	72.1	0.70	0.011	7.7	67.2	5.2
281	10.4	72.1	0.70	0.011	7.7	65.9	5.1
290	10.8	71.5	0.71	0.011	7.8	65.9	5.1
300	11.3	71.3	0.72	0.011	7.9	66.8	5.3
310	12.3	71.3	0.72	0.011	7.9	67.4	5.3
320	13.5	72.6	0.71	0.011	7.8	66.2	5.2
325	14.2	70.4	0.74	0.011	8.1	68.0	5.5

future geotechnical, chemical, and mineralogical analyses on land.

#### 4.1. Stratigraphic control

The stratigraphy of the core was established using Sr isotope ratios of fish teeth (ichthyoliths) following the work of Gleason et al. (2002) (Hyeong et al., 2005). Based on the age–depth curve (Fig. 2a), the converted age increases systematically with increasing depth from 1.1 Ma at 25 cm depth and to 15.5 Ma at 327 cm, with a resolution of  $\pm 1$  Myr for the most intervals. A break in slope in the constructed age–depth curve occurs at 250 cm, corresponding to an age of 7.6 Ma. It indicates different sedimentation rates for the upper and lower intervals. Based on it, the linear sedimentation rates (LSRs) were estimated at  $0.3 \text{ mm}/10^3 \text{ yr}$  in average for the upper interval and  $0.1 \text{ mm}/10^3 \text{ yr}$  in average for the lower interval (Table 1, Fig. 2a).

#### 4.2. Extraction of eolian dust

The inorganic silicate fraction of bulk pelagic sediments, hereafter termed eolian dust, was extracted from the bulk pelagic sediment using a method outlined by Rea and Janecek (1981b). The samples were treated with a 25% acetic acid to remove the carbonate fraction and subsequently with a hot sodium citrate–sodium dithionite solution buffered with sodium bicarbonate to remove Fe–Mn oxides and hydroxides. The solid residue remaining after above two dissolution steps were sieved at  $63 \mu\text{m}$  to

remove coarse biogenic component and then treated with hot sodium carbonate to remove the remaining biogenic silica. The extracted eolian dust samples were freeze-dried for the future analysis and inspected with SEM to make sure of the near complete removal of undesired components.

#### 4.3. Size analyses

The bulk and extracted eolian fractions were treated with hydrogen peroxide to remove organic matter and stored in distilled deionized water with a dispersant (sodium hexametaphosphate) to prevent flocculation. Grain size analysis of the eolian component was carried out between  $0.31$  and  $301 \mu\text{m}$  size intervals using a *Master Sizer Micro* from *Malvern Instrument Inc.* Accuracy of the analysis is  $\pm 2\%$  on volume median diameter. The Master Sizer provides a size distribution by volume, but it can be assumed that the volume distribution represents the corresponding mass distribution because the mineral grains have similar densities. The grain size analysis results are reported as median grain size ( $\phi_{50}$  of Folk, 1974).

#### 4.4. Mass accumulation rate

The mass accumulation rate (MAR), the mass flux of bulk sediment, is the product of the linear sedimentation rate (LSR) and the dry bulk density of the sample. Then, the MAR of eolian fraction was calculated by multiplying the eolian percentage by the determined MAR. The dry bulk density of the sediment (DBD) was calculated from

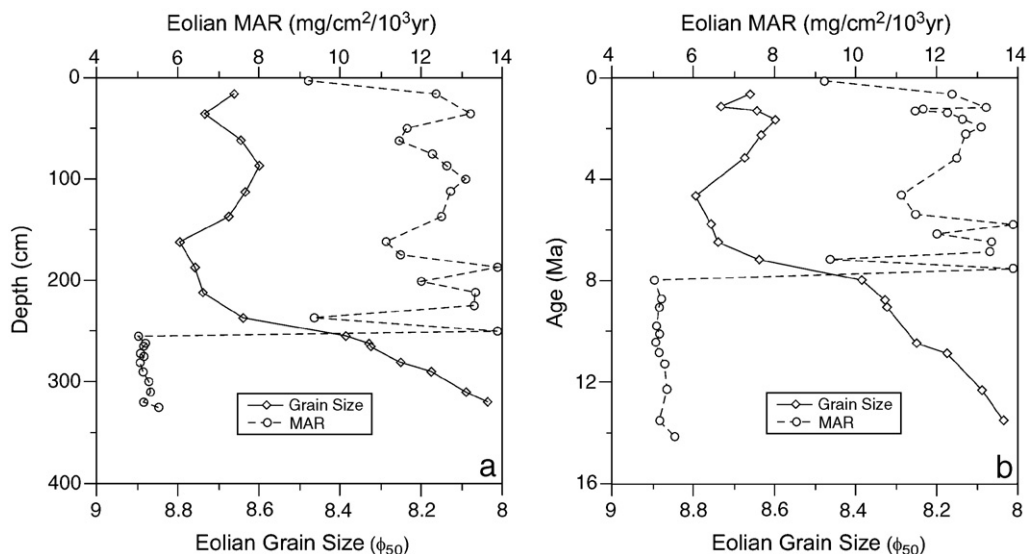


Fig. 3. Plots of grain sizes and mass accumulation rates (MAR) of eolian components against depth (a) and age (b) in the study core.

the determined porosities ( $P$ ) and grain density of sediments ( $\rho$ ) (Table 1) using the relationship of  $P = (1 - P/100) \times \rho$  (Rea and Janecek, 1981b).

## 5. Results

The estimated fluxes of eolian components were low, less than  $14 \text{ mg/cm}^2/10^3 \text{ yr}$  for all the intervals (Fig. 3). However, decreases in eolian MARs are apparent across the 250 cm boundary that separates the upper and lower interval. The eolian MARs of the lower interval are very uniform at  $5 \pm 1 \text{ mg/cm}^2/10^3 \text{ yr}$ , while those of the upper interval vary between 9 and  $14 \text{ mg/cm}^2/10^3 \text{ yr}$  with an average of  $12 \text{ mg/cm}^2/10^3 \text{ yr}$ . There is more than a two-fold increase in the MAR across the 250 cm boundary between the lower and upper intervals. Large variations in eolian MAR are observed in the upper interval. In the 187–250 cm interval (5.8 to 7.6 Ma), eolian MAR increases up to  $14 \text{ mg/cm}^2/10^3 \text{ yr}$ . Above 150 cm interval (from around 4 Ma), eolian MAR increases toward the top of the core from 11 to  $13 \text{ mg/cm}^2/10^3 \text{ yr}$ .

The median grain size of the eolian dusts in the upper interval varies in a narrow range from  $8.8\phi$  ( $2.3 \mu\text{m}$ ) to  $8.6\phi$  ( $2.6 \mu\text{m}$ ) with an average of  $8.7\phi$  ( $2.5 \mu\text{m}$ ) (Table 2, Fig. 3). In contrast, the median grain size of the eolian dusts in the lower interval increases gradually downward from  $8.4\phi$  ( $3.0 \mu\text{m}$ ) at 255 cm depth  $8.0\phi$  ( $3.8 \mu\text{m}$ ) at 320 cm depth. Along with the decrease in the MARs of the eolian dusts, a pronounced change in median grain size is also apparent across the interval boundary

at 250 cm, in which average median grain size increases from  $8.7\phi$  ( $2.5 \mu\text{m}$ ) to  $8.2\phi$  ( $3.5 \mu\text{m}$ ), about a  $0.5\phi$  ( $1 \mu\text{m}$ ) increase, across the interval boundary at 250 cm (Fig. 3, Table 2).

## 6. Discussion

Deep-sea sediments more than 1000 or 2000 km away from the land are devoid of hemipelagic material and contain wind-blown eolian dust as an important non-authigenic, inorganic component (Rea, 1994). The average grain size of eolian dust becomes in equilibrium with the strength of the transporting wind with time and distance (1000–2000 km), and thus reflects the intensity of zonal wind system that carries dust particles beyond the distance of this range (Rea, 1982; Rea and Janecek, 1982; Rea et al., 1985; Rea, 1994; Rea and Hovan, 1995). On the other hand, the mass accumulation rate of wind-borne dust depends mainly on the climate of the source region that controls the availability of dust material (Parkin and Shackleton, 1973; Rea and Janecek, 1981a; Rea, 1982; Rea et al., 1985; Rea, 1994). Thus the pronounced changes in the eolian MARs and grain sizes at 250 cm depth of the study core might be attributed to changes in zonal wind system and availability of eolian material in the source region.

The average of median grain size ( $8.7\phi$ ) of the upper interval is  $0.5\phi$  ( $1 \mu\text{m}$ ) finer than that ( $8.2\phi$ ) of the lower interval, implying decreased zonal wind intensity since about 7.6 Ma, the estimated age for the boundary between the upper and lower intervals (Fig. 3). Furthermore, eolian MARs ( $12 \text{ mg/cm}^2/10^3 \text{ yr}$  in average) of the upper interval are more than 2-times higher than those ( $5 \text{ mg/cm}^2/10^3 \text{ yr}$  in average) of the lower interval, indicative of increased availability of the dust material during the same period of time (Fig. 3).

These pronounced down-core changes in the eolian MARs and grain size can not be explained by climatic change in the source region (wetter conditions in Asia) and stronger westerlies prior to 7.6 Ma under the zonal wind system and provenance same as of today. Two north Pacific cores, LL44-GPC3 and DSDP 576, that have been under the influence of the westerlies and northeast trade winds since 40 Ma (Pettke et al., 2002) show a gradual decrease in both eolian MAR values and grain size with increasing depth and do not show pronounced variation in MAR values and grain size for the past 16 million years (Janecek and Rea, 1983; Janecek, 1985) (Fig. 4). It leads us to consider a possibility of change in both source region and zonal wind system to explain the down-core variation of eolian dust in the study core.

Table 2  
Grain sizes of eolian material in the study core

Depth (cm)	Age (Ma)	Median grain size	
		( $\mu\text{m}$ )	( $\phi$ )
16	0.6	2.5	8.7
36	1.1	2.4	8.7
62	1.3	2.5	8.6
87	1.6	2.6	8.6
112	2.2	2.5	8.6
137	3.2	2.5	8.7
162	4.6	2.3	8.8
187	5.8	2.3	8.8
212	6.5	2.3	8.7
237	7.2	2.5	8.6
255	8.0	3.0	8.4
262	8.7	3.1	8.3
265	9.0	3.1	8.3
281	10.4	3.3	8.3
290	10.8	3.5	8.2
310	12.3	3.7	8.1
320	13.5	3.8	8.0

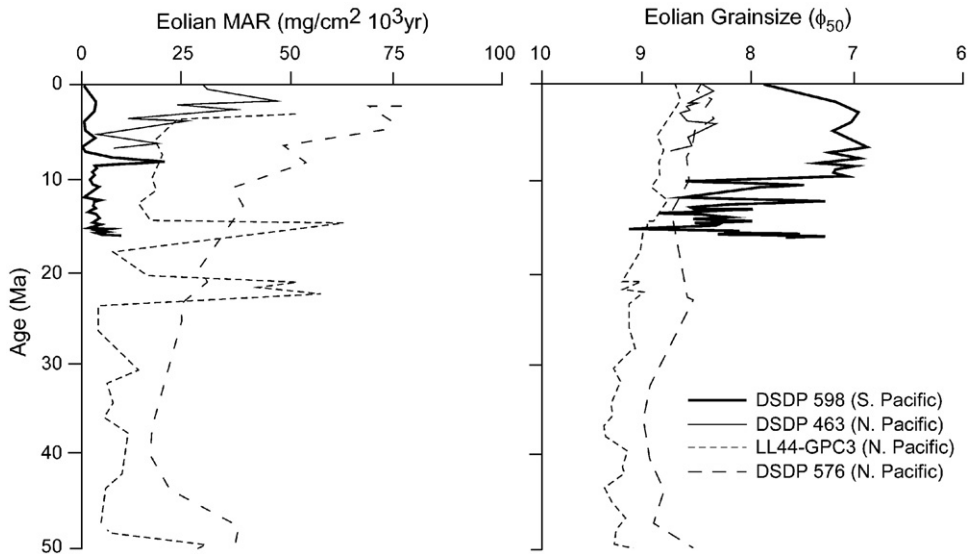


Fig. 4. Mass accumulation rate (MAR) and grain size of eolian components from DSDP 598 (Bloomstine and Rea, 1986), DSDP 463 (Rea and Janecek, 1982), DSDP 576 (Janecek, 1985), and LL44-GPC3 (Janecek and Rea, 1983) cores. Data are from Bloomstine and Rea (1986). Core locations are shown in Fig. 1.

A mineralogical and geochemical study carried out on this same core by Hyeong et al. (2005) supports this possibility. The eolian dusts of the lower interval show a geochemical and mineralogical affinity to equatorial and southeast Pacific surface sediments, and those of the upper interval to north Pacific sediments (Hyeong et al., 2005). Based on the observations, Hyeong et al. (2005) reached a conclusion that eolian dusts of the upper interval were supplied mainly from Asia and those of the lower interval were from Central/South America. Such a source change occurs across the ITCZ as Chinese loess prevails north of the ITCZ while Central/South American dust does south of the ITCZ (Griffin and Goldberg, 1963; Merrill et al., 1989; Nakai et al., 1993; Rea, 1994; Hovan, 1995; Jones et al., 2000; Pettke et al., 2002; Lyle et al., 2002). It indicates that the study site had been under the influence of the southern hemispheric zonal wind system during its earlier depositional period, and subsequently of the northern hemispheric system at a later period when the sediments of upper interval were deposited (Hyeong et al., 2005). If this is the case, the decrease in median grain size and corresponding increase in MARs of the upper interval can be attributed to the same cause.

This interpretation is consistent with the MAR and grain size variations of east Pacific surface sediments encountered across the ITCZ. Dust fluxes of today in the north Pacific, derived from surface sediments (see Fig. 7 in Rea, 1994) and sediment trap experiments (see Fig. 6

in Duce et al., 1991), decline to the east toward North America and to the south toward the ITCZ. Dust fluxes are over  $1000 \text{ mg/cm}^2/10^3 \text{ yr}$  in the northwest Pacific directly downwind from Asia and decrease to less than  $20 \text{ mg/cm}^2/10^3 \text{ yr}$  near the study site north of the ITCZ. They further drop to only  $1\text{--}2 \text{ mg/cm}^2/10^3 \text{ yr}$  in the southeast Pacific because of low availability of dust material in the source region, Central and South America (Duce et al., 1991; Rea, 1994; Rea et al., 1994). The remarkably low dust flux to the southeast Pacific has been maintained at about  $1 \text{ to } 4 \text{ mg/cm}^2/10^3 \text{ yr}$  since the Early to Middle Miocene (Fig. 4) (Bloomstine and Rea, 1986; Rea and Bloomstine, 1986; Rea, 1989). These values are more than two orders of magnitude less than the Plio–Pleistocene fluxes to the north Pacific and more than 3-fold less than the pre-glacial Neogene fluxes observed in LL44-GPC3, DSDP 463, and DSDP 576 cores raised in the north Pacific (Fig. 4, see Fig. 1 for locations) (Rea and Janecek, 1982; Janecek and Rea, 1983; Janecek, 1985; Rea, 1989). The large contrast in dust mass fluxes to pelagic ocean between south and north of the ITCZ has remained at least for the past 16 million years (Fig. 4). The MARs of the upper and lower intervals of core agree well with those of the north and south Pacific in magnitude.

We can draw a similar conclusion from grain size data. When disregarding the coastal areas affected by hemipelagic sedimentation, grain size of eolian dust distributed in the surface of the north Pacific varies in a

narrow range along a west to east transect, from  $8.0\phi$  to  $8.2\phi$  ( $3.9\text{--}3.4\ \mu\text{m}$ ) in the northwestern part to  $8.3\phi$  to  $8.5\phi$  ( $3.2\text{--}2.8\ \mu\text{m}$ ) in the northeastern part (Rea and Hovan, 1995). There are only a few tenths of a  $\phi$  unit decrease in grain size over a nearly 6000 km-long distance. However, eolian grain size of east equatorial Pacific surface sediments, located south of the ITCZ, is coarser than the northern part at  $7.71$  to  $8.33\phi$  ( $3.1\text{--}4.8\ \mu\text{m}$ ) (Rea and Hovan, 1995). The discussed grain size variation observed from north to south of the east Pacific matches well down-core variation of the study core in trend and magnitude.

The large contrast in grain size of eolian dust between south and north of the ITCZ has also remained at least for the past 16 million years (Fig. 4). Mean grain sizes of sediments in the north Pacific core, LL44-GPC3, generally decrease from a maximum value of  $8.6\phi$  at the surface to  $9.0\phi$  at 15 Ma (Fig. 4) (Janecek and Rea, 1983). DSDP 463 showed a similar grain size variation from  $8.4\phi$  to  $8.8\phi$  for the last 7 million years (Fig. 4) (Rea and Janecek, 1982). DSDP 576 core, located at about 4000 km west to the LL44-GPC3, showed down-core grain size variation similar to LL44-GPC3 but  $0.2\phi$  to  $0.5\phi$  coarser than that of the time equivalent horizon in LL44-GPC3, likely due to its proximal location to the source (Fig. 4). The range ( $8.4\phi\text{--}9.0\phi$ ) of eolian grain size variation recorded in these three north Pacific cores includes that ( $8.6\phi\text{--}8.8\phi$ ) of the upper interval of study core.

In contrast, high resolution paleo-environmental study of RC11-210 core, raised from the equatorial Pacific under the influence of southeast trade winds (Fig. 1), showed wide variation in eolian grain size from  $9.30\phi$  ( $1.58\ \mu\text{m}$ ) to  $7.18\phi$  ( $6.9\ \mu\text{m}$ ) for the past 1 million years (Chuey et al., 1987). This core showed an average mean grain size similar to or slightly coarser than those reported by an eolian grain size study of Pacific cores beneath the prevailing westerlies (Core KK7502; Janecek and Rea, 1985, LL44-GPC3; Janecek and Rea, 1983, DSDP 576; Janecek, 1985). Unlike these north Pacific cores, however, RC11-210 showed high down-core fluctuations in mean grain size and much coarser grain size over  $8.0\phi$ , demonstrating the influence of a zonal wind system that is able to supply coarser dust material to the site.

Other southeast Pacific cores, DSDP 597, 598, and 601, also showed median grain size varying from  $7\phi$  to  $8\phi$  at the surface,  $1\phi$  to  $2\phi$  coarser than north Pacific cores. In the DSDP 598 core in which complete grain size data are available back to 16 Ma, the grain size of the eolian dust from sediments younger than 9.5 Ma was uniform at around  $7.2\phi$  (Fig. 4). Sediments older than 9.5 Ma exhibited the reduced grain size of  $8.2\phi$  on average with rather wide variation from  $7.2\phi$  to  $9.0\phi$

(Fig. 4). The grain sizes of eolian dust in the lower interval of the study core are slightly finer than those of the southeast Pacific cores, but bracketed by the grain size range observed in the southeast Pacific cores.

Eolian MARs and grain sizes of the study core compare well to north Pacific cores in the upper interval above 250 cm, and to equatorial and southeast Pacific cores in the lower interval. It indicates that the study site had been under the influence of southern hemispheric zonal wind system at its earlier depositional period and subsequently of the northern hemispheric system at a later period when the upper interval was deposited. These results support the conclusion drawn from the mineralogical and geochemical study assigning the source of the upper and lower intervals to Asia and Central/South America, respectively. Furthermore, this interpretation is consistent with the geologic history of the ITCZ moving southward toward the geographical equator through the Neogene from its prior northerly position (Rea, 1994; Lyle et al., 2002; Pettke et al., 2002). This study suggests that distinct MAR and grain size difference in eolian components of Pacific sediments south and north of the ITCZ are recorded in deep-sea cores and can be used to trace the paleo-location of the ITCZ, alone or along with geochemical and mineralogical characteristics.

In addition, the study core might also record the northerly passage of this core beneath the Late Miocene ITCZ. It is known that eolian flux increases beneath the ITCZ compared to the north and south because of effective wet-depositional scavenging of aerosol particles associated with high rainfall rates (Hovan, 1995). Thus, the increased eolian MAR values of the 187–250 cm interval from 5.8 to 7.6 Ma, right above the interval that marks the change in source regime, likely represent the interval when the study site was beneath the ITCZ. If this is the case, it indicates a possibility that the ITCZ was located further north at  $\sim 13^\circ\text{N}$  during the Late Miocene,  $1^\circ$  north to the paleo-latitude of  $12^\circ\text{N}$  proposed by Hyeong et al. (2005) using the same core.

Meanwhile, the study core also shows the increase in eolian MAR value above 150 cm interval (from  $\sim 4$  Ma). It might be attributed to drier northern hemisphere continents and slightly stronger atmospheric circulation associated with the late Cenozoic northern hemisphere cooling that began 3.5 Ma (Rea and Janecek, 1982; Rea et al., 1988; Rea, 1994).

There is a concern about direct comparison of grain size data because of slight discrepancies in results produced from different analyzer systems. However, published data clearly show clear distinction in grain size variation across the ITCZ and good agreement with our

data in magnitude. Thus, it can be assumed that the differences in grain size distribution of eolian dust across the ITCZ are real and large enough to overcome inter-instrumental errors. It indicates that grain size variation can be used as a proxy for geographical location relative to the ITCZ.

## 7. Conclusions

The mass fluxes and grain sizes of eolian components are distinctly different in the lower and upper intervals of the study core. The eolian MARs of the lower interval are very uniform at  $5 \pm 1 \text{ mg/cm}^2/10^3 \text{ yr}$ , while those of the upper interval are more than 2 times higher than the lower interval at  $12 \pm 1 \text{ mg/cm}^2/10^3 \text{ yr}$ . The median grain size of the eolian dusts in the lower interval increases gradually downward from  $8.4\phi$  ( $3.0 \mu\text{m}$ ) at 255 cm depth to  $8.0\phi$  ( $3.8 \mu\text{m}$ ) at 320 cm depth. Those of the upper interval vary in a narrow range from  $8.8\phi$  ( $2.3 \mu\text{m}$ ) to  $8.6\phi$  ( $2.6 \mu\text{m}$ ). There is about  $0.5\phi$  ( $1 \mu\text{m}$ ) down-core increase in median grain size across the interval boundary at 250 cm.

Eolian MAR and grain size variation of the study core compare well to north Pacific cores in the upper interval above 250 cm, and to the equatorial and south-east Pacific cores in the lower interval. It indicates that the study site had been under the influence of southern hemispheric zonal wind system at its earlier depositional period and subsequently of the northern hemispheric system at a later period during which the upper interval was deposited. These results support the conclusion drawn from the mineralogical and geochemical study assigning the source of the upper and lower intervals to Asia and Central/South America, respectively (Hyeong et al., 2005). This interpretation is consistent with the geologic history of the ITCZ moving southward toward the geographical equator through the Neogene from its prior northerly position (Rea, 1994; Lyle et al., 2002; Pettke et al., 2002). This study suggests that distinct MAR and grain size difference in eolian components of Pacific sediments south and north of the ITCZ are recorded in deep-sea cores and can be used to trace the paleo-location of the ITCZ, alone or along with geochemical and mineralogical characteristics.

## Acknowledgments

This project was funded by the Ministry of Maritime Affairs and Fisheries, Republic of Korea and partly by Korea Ocean Research and Development Institute (PE896-00 and PE939-00). We thank H. B. Lee for his aid in sample preparation and treatment. We also

thank David K. Rea and Jan-Berend Stuut for helpful comments that significantly improved the manuscript.

## References

- Biscaye, P.E., 1965. Mineralogy and sedimentation of recent deep-sea clay in the Atlantic ocean and adjacent seas and oceans. *Geol. Soc. Amer. Bull.* 76, 803–831.
- Bloomstine, M.K., Rea, D.K., 1986. Post-middle Oligocene eolian deposition from the trade winds of the southeast Pacific. *Initial Rep. Deep Sea Drill. Proj.* 92, 331–340.
- Chuey, J.M., Rea, D.K., Pisias, N.G., 1987. Late Pleistocene paleoclimatology of the central Equatorial Pacific: a quantitative record of eolian and carbonate deposition. *Quat. Res.* 28, 323–339.
- Corliss, B.H., Hollister, C.D., et al., 1982. A paleoenvironmental model for Cenozoic sedimentation in the central North Pacific. In: Scrutton, R.A., Talwani, M. (Eds.), *The Ocean Floor*. J. Wiley and Sons Ltd., pp. 277–304.
- Duce, R.A., et al., 1991. The atmospheric input of trace species to the world ocean. *Glob. Biogeochem. Cycles* 5, 193–259.
- Flohn, H., 1981. A hemispheric circulation asymmetry during late Tertiary. *Geol. Rundsch.* 70, 725–736.
- Folk, R.L., 1974. *Petrology of Sedimentary Rocks*. Hemphill, Austin, TX.
- Gleason, J.D., Moore, T.C., Rea, D.K., Johnson, T.M., Owen, R.M., Blum, J.D., Hovan, S.A., Jones, C.E., 2002. Ichthyolith strontium isotope stratigraphy of a Neogene red clay sequence: calibrating eolian dust accumulation rates in the central North Pacific. *Earth Planet. Sci. Lett.* 202, 625–636.
- Griffin, J.J., Goldberg, E.D., 1963. Clay-mineral distribution in the Pacific Ocean. In: Hill, M.N. (Ed.), *The Sea*, vol. 3. Interscience, New York, pp. 728–741.
- Hay, W.W., DeConto, R., Wold, C.N., Wilson, K.M., Voigt, S., Schulz, M., Wold-Rosby, A., Dullo, W.-C., Ronov, A.B., Balukhovskiy, A.N., Soeding, E., 1999. Alternative Global Cretaceous Paleogeography. In: Barrera, E., Johnson, C. (Eds.), *The Evolution of Cretaceous Ocean/Climate Systems*. *Geol. Soc. Am. Sp. Papers*, vol. 332, pp. 1–47.
- Hovan, S.A., 1995. Late Cenozoic atmospheric circulation intensity and climatic history recorded by eolian deposition in the eastern equatorial Pacific ocean, Leg 138. *Proc. Ocean Drill. Program Sci. Results* 139, 615–625.
- Hyeong, K., Park, S.-H., Yoo, C.M., Kim, K.-H., 2005. Mineralogical and geochemical compositions of the eolian dust from the northeast equatorial Pacific and their implications on paleolocation of the Intertropical Convergence Zone. *Paleoceanography* 20, PA1010. doi:10.1029/2004PA001053.
- Janecek, T.R., 1985. Eolian sedimentation in the northwest Pacific Ocean: a preliminary examination of the data from Deep Sea Drilling Project sites 576 and 578. *Initial Rep. Deep Sea Drill. Proj.* 86, 589–603.
- Janecek, T.R., Rea, D.K., 1983. Eolian deposition in the northeast Pacific Ocean: Cenozoic history of atmospheric circulation. *Geol. Soc. Amer. Bull.* 94, 730–738.
- Janecek, T.R., Rea, D.K., 1985. Quaternary fluctuations in northern hemisphere tradewinds and westerlies. *Quat. Res.* 24, 150–163.
- Jeong, K.S., Kang, J.K., Chough, S.K., 1994. Sedimentary processes and manganese nodule formation in the Korea Deep Ocean Study (KODOS) area, western part of Clarion–Clipperton fracture zones, northeast equatorial Pacific. *Mar. Geol.* 122, 122–150.
- Jones, C.E., Halliday, A.N., Rea, D.K., Owen, R.M., 1994. Neodymium isotopic variations in north Pacific modern silicate

- sediment and the insignificance of detrital REE contributions to seawater. *Earth Planet. Sci. Lett.* 127, 55–66.
- Jones, C.E., Halliday, A.N., Rea, D.K., Owen, R.M., 2000. Eolian inputs of lead to the north Pacific. *Geochim. Cosmochim. Acta* 64, 1405–1416.
- Jung, H.S., Lee, C.B., Jeong, K.S., Kang, J.K., 1998. Geochemical and mineralogical characteristics in two-color core sediments from the Korea Deep Ocean Study (KODOS) area, northeast equatorial Pacific. *Mar. Geol.* 144, 295–309.
- Kyte, F.T., Leinen, M., Heath, G.R., Zhou, L., 1993. Cenozoic sedimentation history of the central north Pacific: inferences from the elemental geochemistry of core LL44-GPC3. *Geochim. Cosmochim. Acta* 57, 1719–1740.
- Lyle, M., Wilson, P.A., Janecek, T.R., et al., 2002. Leg 199 Summary. *Proc. Ocean Drill. Program: Initial Rep.* 199, 1–87.
- Merrill, J.T., Uematsu, M., Bleck, R., 1989. Meteorological analysis of long range transport of mineral aerosols over the north Pacific. *J. Geophys. Res.* 94, 8584–8598.
- Muller, P.J., Mangini, A., 1980. Organic carbon decomposition rates in sediments of the Pacific manganese nodule belt dated by Th-230 and Pa-231. *Earth Planet. Sci. Lett.* 51, 94–114.
- Muller, P.J., Hartmann, M., Suess, E., 1988. Environment of manganese nodules. In: Halbach, P., Friedrich, G., von Stackelberg, U. (Eds.), *The Manganese Nodule Belt of the Pacific Ocean*. Ferdinand Enke Verlag, Stuttgart, pp. 70–141.
- Nakai, S., Halliday, A.N., Rea, D.K., 1993. Provenance of dust in the Pacific ocean. *Earth Planet. Sci. Lett.* 119, 143–157.
- Olivarez, A.M., Owen, R.M., Rea, D.K., 1991. Geochemistry of eolian dust in Pacific pelagic sediments: implications for paleoclimatic interpretations. *Geochim. Cosmochim. Acta* 55, 2147–2158.
- Parkin, D.W., Shackleton, N.J., 1973. Trade wind and temperature correlations down a deep-sea core off the Saharan Coast. *Nature* 245, 455–457.
- Pettke, T., Halliday, A.N., Rea, D.K., 2002. Cenozoic evolution of Asian climate and sources of Pacific seawater Pb and Nd derived from eolian dust of sediment core LL44-GPC3. *Paleoceanography* 17, 3-1–3-13.
- Piper, D.Z., Blueford, J.R., 1982. Distribution, mineralogy, and texture of manganese nodules and their relation to sedimentation at DOMES site A in the equatorial north Pacific. *Deep-Sea Res.* 29, 927–952.
- Piper, D.Z., Williamson, M.E., 1977. Composition of Pacific ocean ferromanganese nodules. *Mar. Geol.* 123, 285–303.
- Piper, D.Z., Cook, H.E., Gardner, J.V., 1979. Lithic and acoustic stratigraphy of the equatorial north Pacific: DOMES sites A, B, and C. In: Bischoff, L.L., Piper, D.Z. (Eds.), *Marine Geology and Oceanography of the Pacific Manganese Nodule Province*. Marine Science, vol. 9. Plenum Press, New York, pp. 309–348.
- Pisias, N.G., Mix, A.C., 1997. Spatial and temporal oceanographic variability of the eastern equatorial Pacific during the late Pleistocene: evidence from Radiolaria microfossils. *Paleoceanography* 12, 381–393.
- Rea, D.K., 1982. Fluctuation in eolian sedimentation during the past five glacial–interglacial cycles: a preliminary examination of data from DSDP Site 503B, eastern equatorial Pacific Ocean. *Initial Rep. Deep Sea Drill. Proj.* 62, 661–668.
- Rea, D.K., 1989. Geologic record of atmospheric circulation on tectonic time scales. In: Leinen, M., Sarnthein, M. (Eds.), *Paleoclimatology and Paleometeorology: Modern and Past Patterns of Global Atmospheric Transport*. Kluwer Academic, Norwell, Mass, pp. 841–857.
- Rea, D.K., 1994. The paleoclimatic record provided by eolian deposition in the deep sea: The geologic history of win. *Rev. Geophys.* 32, 159–195.
- Rea, D.K., Bloomstine, M.K., 1986. Neogene history of the South Pacific tradewinds: Evidence for hemispheric asymmetry of atmospheric circulation. *Palaeogeogr. Palaeoclimatol. Palaeoecol.* 55, 55–64.
- Rea, D.K., Hovan, S.A., 1995. Grain size distribution and depositional processes of the mineral component of abyssal sediments: Lessons from the north Pacific. *Paleoceanography* 10, 251–258.
- Rea, D.K., Janecek, T.R., 1981a. Late Cretaceous history of eolian deposition in the Mid-Pacific Mountains, central north Pacific Ocean. *Palaeogeogr. Palaeoclimatol. Palaeoecol.* 36, 55–67.
- Rea, D.K., Janecek, T.R., 1981b. Mass-accumulation rates of the non-authigenic inorganic crystalline (eolian) component of deep-sea sediments from the western mid-Pacific Mountains. *Initial Rep. DSDP* 62, 652–659.
- Rea, D.K., Janecek, T.R., 1982. Late Cenozoic changes in atmospheric circulation deduced from north Pacific eolian sediments. *Mar. Geol.* 49, 149–167.
- Rea, D.K., Hovan, S.A., Janecek, T.R., 1985. Geologic approach to the long term history of atmospheric circulation. *Science* 227, 721–725.
- Rea, D.K., Sooecks, H., Joseph, L.H., 1988. Late Cenozoic eolian deposition in the north Pacific: Asian drying, Tibetan uplift, and cooling of the northern hemisphere. *Paleoceanography* 13, 215–224.
- Rea, D.K., Hovan, S.A., Janecek, T.R., 1994. Late Quaternary flux of eolian dust to the pelagic ocean. In: Hay, W.W. (Ed.), *Material Fluxes on the Surface of the Earth*. National Research Council. National Academy Press, Washington, D.C., pp. 116–124.
- Theyer, F., 1977. Micropaleontological dating of DOMES project box cores from test area A and B, tropical Pacific. In: Piper, D.Z., et al. (Eds.), *Geology and Geochemistry of DOMES Site A, B, and C, Equatorial North Pacific*. US Geol. Surv., Open-file Report, vol. 77–778, pp. 179–194.
- Vanden Berg, M.D., Jarrard, R.D., 2004. Cenozoic mass accumulation rates in the equatorial Pacific based on high-resolution mineralogy of Ocean Drilling Program Leg 199. *Paleoceanography* 19, PA2021. doi:10.1029/2003PA000928.
- Weber II, E.T., Owen, R.M., Kickens, G.R., Halliday, A.N., Jones, C.E., Rea, D.K., 1996. Quantitative resolution of continental eolian material and volcanic ash in north Pacific surface sediment. *Paleoceanography* 11, 115–127.
- Wyrski, K., Kilonsy, B., 1984. Mean water and current structure during the Hawaii-to-Tahiti shuttle experiment. *J. Phys. Oceanogr.* 14, 242–254.